Mathematical Analysis and Simulations of the Neural Circuit for Locomotion in Lampreys

Li Zhaoping,[1] Alex Lewis,[1] and Silvia Scarpetta[2]

[1]*University College, London, United Kingdom*
[2]*INFM & Department of Physics, University of Salerno, Italy*

We analyze the dynamics of the neural circuit of the lamprey central pattern generator. This analysis provides insight into how neural interactions form oscillators and enable spontaneous oscillations in a network of damped oscillators, which were not apparent in previous simulations or abstract phase oscillator models. We also show how the different behavior regimes (characterized by phase and amplitude relationships between oscillators) of forward or backward swimming, and turning, can be controlled using the neural connection strengths and external inputs.

     PACS numbers: 87.19.La, 87.19.St

Locomotion in vertbebrates (walking, swimming, etc.) is generated by central pattern generators (CPGs) in the spinal cord. The CPG for swimming in lampreys is one of the best known [1,2], and has been a model system for investigations. It produces left-right antiphase oscillatory neural and motor activities propagating along a body composed of around 100 segments. A head-to-tail negative or positive oscillation phase gradient, of about 1% of an oscillation cycle per segment, gives forward or backward swimming, respectively, and one wavelength from head to tail. External inputs from the brain stem switch the CPG between forward and backward swimming of various speeds and turning. Since isolated sections of the spinal cord, down to 2–3 segments long [2], can produce swimminglike activity, the oscillations are thought to be generated by the neurons within the CPG. The neural circuit responsible is shown topologically in Fig. 1. It has ipsilaterally projecting excitatory ($\mathbf{E}$) neurons and inhibitory ($\mathbf{L}$) neurons, and contralaterally projecting inhibitory ($\mathbf{C}$) neurons, and provides output to motor neurons via the $\mathbf{E}$ neurons. All neurons project both intra- and intersegmentally. The projection distances are mainly within a few segments, especially from $\mathbf{E}$ and $\mathbf{C}$ neurons, and are longer, and possibly stronger, in the head-to-tail or descending direction [1–3].

Previous analytical work [4,5] mainly treated the CPG as a chain of coupled phase oscillators in a general form $\dot{\theta}_i = \omega_i + \sum_j f_{ij}(\theta_i, \theta_j)$. Here θ_i is the oscillation phase and ω_i the intrinsic frequency of one segment, and $f_{ij}(\theta_i, \theta_j)$ the intersegment coupling. This approach provided important insight into the conditions for phase-locked solutions in general systems of coupled oscillators. However, its generality obscures the roles of specific neural types and their connections in generating and controlling behavior. More recently, bifurcation analysis of the dynamics of a single segment was carried out, for a phase oscillator model derived from a kinetic (Hodgkin-Huxley) equation for neurons [6], and for a neural circuit model similar to the one used in this Letter [7]. Extensive

simulations, including all neural types and detailed neural properties, have reproduced many features of experimental data [1], though their complexity limits further understanding.

In all previous approaches, it is assumed that a single segment in the CPG can oscillate spontaneously, contrary to experimental evidence that at least 2–3 segments are needed for oscillations [2]. We present an analytical study, confirmed by simulations, of a model of the CPG neural circuit in which an isolated single segment has a stable fixed point, with spontaneous oscillations occurring only in chains of coupled segments. The phase oscillator approach is not applicable here since it assumes spontaneously oscillating individual segments perturbed by intersegment coupling. Including specific cell types and their connections enables us to analyze the role of each of them in generating and controlling swimming. We show how external inputs select forward and backward swimming, by controlling the effective strengths of connections between various neurons, and produces turning, by additional input to one side of the CPG only. We also analyze behavior near the body ends.

We model the CPG neural circuit with $N = 100$ segments denoted by $i = 1, \ldots, N$. The vector states $(\mathbf{E}_l, \mathbf{L}_l, \mathbf{C}_l)$ and $(\mathbf{E}_r, \mathbf{L}_r, \mathbf{C}_r)$, modeling the membrane potentials of the local populations of neurons at the left and right side of the body, respectively, with $\mathbf{E}_l = (E_l^1, E_l^2, \ldots, E_l^N)$ etc., are modeled as leaky integrators of their inputs:
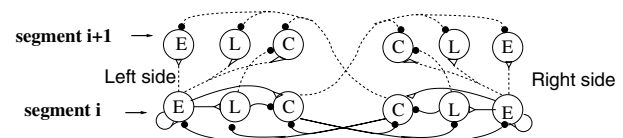

FIG. 1. The lamprey CPG circuit. The solid lines and the dashed lines denote intrasegment and intersegment connections, respectively.

$$\dot{\mathbf{E}}_l = -\mathbf{E}_l - \mathsf{K}^0 g_C(\mathbf{C}_r) + \mathsf{J}^0 g_E(\mathbf{E}_l) + \mathbf{I}_{E,l},$$

$$\dot{\mathbf{L}}_l = -\mathbf{L}_l - \mathsf{A}^0 g_C(\mathbf{C}_r) + \mathsf{W}^0 g_E(\mathbf{E}_l) + \mathbf{I}_{L,l}, \qquad (1)$$

$$\dot{\mathbf{C}}_l = -\mathbf{C}_l - \mathsf{B}^0 g_C(\mathbf{C}_r) + \mathsf{Q}^0 g_E(\mathbf{E}_l) - \mathsf{H}^0 g_L(\mathbf{L}_l) + \mathbf{I}_{C,l},$$

with the same equation for swapped subscripts ($l \leftrightarrow r$). $g_E(\mathbf{E}_l) = (g_E(E_l^1), \dots, g_E(E_l^N))$ are the neural activities or firing rates, as non-negative (sigmoidlike) activation functions of $\mathbf{E}_l$, and likewise for $g_C(\mathbf{C}_l)$ and $g_L(\mathbf{L}_l)$. K^0, J^0, A^0, W^0, B^0, Q^0, and H^0 are $N \times N$ matrices of non-negative synaptic strengths between neurons. $\mathbf{I}_{E,l}$, $\mathbf{I}_{L,l}$, and $\mathbf{I}_{C,l}$ are external inputs, including those from the brain stem, assumed to be static. A left-right symmetric fixed point $(\bar{\mathbf{E}}, \bar{\mathbf{L}}, \bar{\mathbf{C}})$ where $(\dot{\mathbf{E}}, \dot{\mathbf{L}}, \dot{\mathbf{C}}) = 0$ exists with external inputs $\mathbf{I}_{E,l} = \bar{\mathbf{E}}_l + \mathsf{K}^0 g_C(\bar{\mathbf{C}}_r) - \mathsf{J}^0 g_E(\bar{\mathbf{E}}_l)$ (and analogously for other $\mathbf{I}$'s). Dynamics for small deviations from $(\bar{\mathbf{E}}, \bar{\mathbf{L}}, \bar{\mathbf{C}})$ can be approximated linearly, and, with a coordinate rotation $(\mathbf{E}_\pm, \mathbf{L}_\pm, \mathbf{C}_\pm) \equiv [(\mathbf{E}_l, \mathbf{L}_l, \mathbf{C}_l) - (\bar{\mathbf{E}}, \bar{\mathbf{L}}, \bar{\mathbf{C}})] \pm [(\mathbf{E}_r, \mathbf{L}_r, \mathbf{C}_r) - (\bar{\mathbf{E}}, \bar{\mathbf{L}}, \bar{\mathbf{C}})]$, transformed into two decoupled modes — the left-right synchronous mode $(\mathbf{E}_+, \mathbf{L}_+, \mathbf{C}_+)$ and the antiphase mode $(\mathbf{E}_-, \mathbf{L}_-, \mathbf{C}_-)$. Swimming entails $(\mathbf{E}_-, \mathbf{L}_-, \mathbf{C}_-)$ oscillating with a wavelength of one body length, while $\mathbf{E}_+, \mathbf{L}_+, \mathbf{C}_+$ is damped. The linearized equations are

$$\dot{\mathbf{E}}_\pm = -\mathbf{E}_\pm \mp \mathsf{K}\mathbf{C}_\pm + \mathsf{J}\mathbf{E}_\pm,$$

$$\dot{\mathbf{L}}_\pm = -\mathbf{L}_\pm \mp \mathsf{A}\mathbf{C}_\pm + \mathsf{W}\mathbf{E}_\pm, \qquad (2)$$

$$\dot{\mathbf{C}}_\pm = -\mathbf{C}_\pm \mp \mathsf{B}\mathbf{C}_\pm + \mathsf{Q}\mathbf{E}_\pm - \mathsf{H}\mathbf{L}_\pm,$$

where $\mathsf{K} \equiv \mathsf{K}^0 g_C'(\bar{\mathbf{C}})$, $\mathsf{A} \equiv \mathsf{A}^0 g_C'(\bar{\mathbf{C}})$, $\mathsf{B} \equiv \mathsf{B}^0 g_C'(\bar{\mathbf{C}})$, $\mathsf{J} \equiv \mathsf{J}^0 g_E'(\bar{\mathbf{E}})$, $\mathsf{W} \equiv \mathsf{W}^0 g_E'(\bar{\mathbf{E}})$, $\mathsf{Q} \equiv \mathsf{Q}^0 g_E'(\bar{\mathbf{E}})$, and $\mathsf{H} \equiv \mathsf{H}^0 g_L'(\bar{\mathbf{L}})$ are effective connection matrices, and the $g'(\cdots)$'s denote derivatives. The $\mathbf{C}$ neurons thus become effectively excitatory in the antiphase mode. Noting that the lengths of the neural connections are much shorter than the body, and that isolated sections of the spinal cord from any part of the body generate oscillations with similar amplitude and phase relationships [1,2], we make the approximation of translation invariance, so that matrix elements such as J_{ij} depend only on $(i - j)$, and impose the periodic boundary condition, $\mathsf{J}_{ij} = \mathsf{J}(x)$, where $x = (i - j) \bmod N$. This is adequate when behavior near body ends is not considered. Then all connection matrices commute with each other, with common eigenvectors (expressed as functions of segment number x) $[\mathbf{E}(x), \mathbf{L}(x), \mathbf{C}(x)] \propto e^{i(2\pi m/N)x}$ for integer eigenmode $-N/2 < m \le N/2$. The system solutions are thus combinations of modes $[\mathbf{E}_\pm(x, t), \mathbf{L}_\pm(x, t), \mathbf{C}_\pm(x, t)] \propto e^{\lambda_m^\pm t + i(2\pi m/N)x}$, where $\lambda_m^\pm$ is the eigenvalue of Eq. (2) for mode m. Forward swimming results if the real part $\mathrm{Re}(\lambda_m^\pm) < 0$ for all modes except the antiphase mode with $m = 1$, i.e., $\mathrm{Re}(\lambda_1^-) > 0$. Then this mode dominates the solution (whose growing amplitude will be constrained by nonlinearity) $[\mathbf{E}(x, t), \mathbf{L}(x, t), \mathbf{C}(x, t)] \propto e^{\mathrm{Re}(\lambda_1^-)t - i(\omega t - kx)}$, with oscillation frequency $\omega \equiv |\mathrm{Im}(\lambda_1^-)|$ and wave number $k = 2\pi/N$. Using the convention $e^{-i\omega t}$ for oscillations, we omitted the solution

$\propto e^{\mathrm{Re}(\lambda_1^-)t + i\omega t}$ in the conjugate pair of eigenvalues. To simplify our system, we note from experimental data that, in forward swimming, $\mathbf{E}$ and $\mathbf{L}$ oscillate roughly in phase within a segment, while $\mathbf{C}$ leads them [2]. We scale our variable definitions so that $\mathbf{E}_- = \mathbf{L}_-$ in forward swimming. Then Eq. (2) implies that $(\mathsf{K} - \mathsf{A})\mathbf{C}_- = -(\mathsf{J} - \mathsf{W})\mathbf{E}_-$ in forward swimming. Since $\mathbf{E}$ and $\mathbf{C}$ have much shorter connections than the wavelength of oscillations during swimming, the connection matrices have zero elements far from the diagonal, making $(\mathsf{K} - \mathsf{A})\mathbf{C}_-$ and $(\mathsf{J} - \mathsf{W})\mathbf{E}_-$ roughly either in phase or in antiphase with $\mathbf{C}_-$ and $\mathbf{E}_-$, respectively. As $\mathbf{C}_-$ phase leads $\mathbf{E}_-$, $(\mathsf{K} - \mathsf{A})\mathbf{C}_- = -(\mathsf{J} - \mathsf{W})\mathbf{E}_-$ is impossible unless $(\mathsf{J} - \mathsf{W})\mathbf{E}_- = (\mathsf{K} - \mathsf{A})\mathbf{C}_- = 0$. For simplicity we henceforth assume $\mathsf{J} = \mathsf{W}$ and $\mathsf{K} = \mathsf{A}$, since nonswimming modes do not concern us. Consequently $\mathbf{E}_\pm = \mathbf{L}_\pm$ and

$$\begin{pmatrix} \dot{\mathbf{E}}_\pm \\ \dot{\mathbf{C}}_\pm \end{pmatrix} = \begin{pmatrix} \mathsf{J} - 1 & \mp\mathsf{K} \\ -(\mathsf{H} - \mathsf{Q}) & \mp\mathsf{B} - 1 \end{pmatrix} \begin{pmatrix} \mathbf{E}_\pm \\ \mathbf{C}_\pm \end{pmatrix}, \qquad (3)$$

where $\mathbf{L}$ and $\mathbf{E}$ are treated as a single population inhibiting or exciting $\mathbf{C}$ via connections $\mathsf{H} - \mathsf{Q}$. The eigenvalues for mode m are

$$\lambda_m^+ = [-2 + J_m - B_m \pm \sqrt{R_m + 2(B_m^2 + J_m^2)}]/2,$$
$$\lambda_m^- = [-2 + J_m + B_m - i\sqrt{R_m}]/2. \qquad (4)$$

$J_m \equiv \sum_x \mathsf{J}(x) e^{-i(2\pi m/N)x}$ is the eigenvalue of J (and analogously for other matrices), and R_m is the eigenvalue of $\mathsf{R} \equiv 4\mathsf{K}(\mathsf{H} - \mathsf{Q}) - (\mathsf{B} - \mathsf{J})^2$.

To elucidate the conditions needed for the antiphase mode with $m = \pm 1$ for forward or backward swimming to dominate, we analyze the bifurcations which occur as $\lambda_m^\pm$ for each mode $(m, \pm)$ changes as the effective neural connections are varied, either directly or via the external inputs. First, we focus on the left-right mode space (as in [6,7] for a single segment) of $+$ and $-$, i.e., the synchronous and antiphase modes, by simply taking $m = 0$. Then, J_0, B_0, H_0, K_0, and Q_0, are all real and nonnegative, each being the total connection strength on a postsynaptic cell from all cells of a particular type. Oscillation in the antiphase mode requires $R_0 > 0$, necessitating $H_0 > Q_0$, or that, in the ac component of interactions above the background dc level, $\mathbf{C}$ neurons receive stronger inhibition from $\mathbf{L}$ neurons than excitation from $\mathbf{E}$ neurons. Consequently, λ_0^+ is real and the synchronous mode is nonoscillatory. As neural connections increase from zero, the antiphase mode undergoes a Hopf bifurcation when $\mathrm{Re}(\lambda_0^-) = 0$, at $J_0 + B_0 = 2$, and the synchronous mode undergoes a pitchfork bifurcation when $\lambda_0^+ = 0$, at $(B_0 + 1)(1 - J_0) = K_0(H_0 - Q_0)$. Oscillations result if the Hopf bifurcation has occurred but the pitchfork bifurcation has not, i.e., $\mathrm{Re}(\lambda_0^-) > 0 > \lambda_0^+$. The condition $\lambda_0^+ < 0$ implies $(B_0 + 1)(1 - J_0) > K_0(H_0 - Q_0)$, necessitating $J_0 < 1$. Meanwhile, $\mathrm{Re}(\lambda_0^-) > \lambda_0^+$ leads to $B_0 > \sqrt{J_0^2 + R_0/2} > J_0$, thus requiring sufficient inhibitory connections between left and right $\mathbf{C}$ cells.

The J, W, and Q connections from **E** cells have to be relatively weak, consistent with the findings of [7].

Assuming the synchronous mode is damped, we focus now on the antiphase mode in the m mode space. Hopf bifurcations occur sequentially in various modes m in the order of descending $\mathrm{Re}(\lambda_m^-)$. Taylor expanding J_m (and similarly B_m, R_m) for small wave number $k = 2\pi m/N$ as is relevant for swimming, $J_m = j_0 - ikj_1 - k^2 j_2 + \mathcal{O}(k^3)$ with $j_n = \sum_x \mathsf{J}(x)\frac{x^n}{n!}$, we have

$$2\mathrm{Re}[\lambda^-(k)] = -2 + j_0 + b_0 - kr_1/(2\sqrt{r_0})$$
$$- k^2(j_2 + b_2) + \mathcal{O}(k^3),$$
$$2\mathrm{Im}[\lambda^-(k)] = \sqrt{r_0} + \mathcal{O}(k), \tag{5}$$

making the mode with $k \approx -r_1/[4\sqrt{r_0}(j_2 + b_2)]$ dominant with the largest $\mathrm{Re}[\lambda^-(k)]$. From the definition, $(r_0, j_2, b_2) \geq 0$, while stronger and/or longer connections in the descending direction imply $(j_1, b_1) > 0$. Simply, J (and similarly for other matrices) is said to be descending (or ascending) if $j_1 > 0$ (or $j_1 < 0$). Hence, if R is ascending, i.e., $r_1 < 0$, $\mathrm{Re}[\lambda^-(k)]$ increases with increasing k, and the dominant wave number can be set to $k = 2\pi/N$ for mode $m = 1$ by tuning the values of R, J, and B. If the connection strengths are such that only the $m = 1$ mode undergoes the Hopf bifurcation, forward swimming emerges spontaneously. Switching R to descending leads to backward swimming. Note that J, B, H, K, and Q are all descending, multiplications and summations of descending connections are still descending, and negating a descending connection makes it ascending. Since B and H have to dominate J and Q, respectively, R is composed of an ascending term $-(\mathsf{B} - \mathsf{J})^2$ and a descending term $4\mathsf{K}(\mathsf{H} - \mathsf{Q})$. Depending on the relative strengths of these two terms, R can be ascending or descending to achieve forward or backward swimming. This could be achieved by changing the static inputs to shift the fixed point $(\bar{\mathbf{E}}, \bar{\mathbf{L}}, \bar{\mathbf{C}})$ of the system to a different gain regime $g_E'(\bar{\mathbf{E}})$, $g_L'(\bar{\mathbf{L}})$, $g_C'(\bar{\mathbf{C}})$, and thus different effective connection strengths $\mathsf{H} = \mathsf{H}^0 g_L'(\bar{\mathbf{L}})$, etc., without changing the underlying strengths H^0, etc. Alternatively, the external inputs might recruit extra functional cells to alter the effective connection strengths [8].

When additional modes satisfy $\mathrm{Re}(\lambda_m^-) > 0$, the dynamics depends on the nonlinear coupling between modes. For illustration, consider nonlinearity only in $g_C(\mathbf{C})$.

$$\dot{\mathbf{E}}_\pm = -\mathbf{E}_\pm \mp \mathsf{K}^0 g_\pm(\mathbf{C}) + \mathsf{J}\mathbf{E}_\pm,$$
$$\dot{\mathbf{L}}_\pm = -\mathbf{L}_\pm \mp \mathsf{A}^0 g_\pm(\mathbf{C}) + \mathsf{W}\mathbf{E}_\pm, \tag{6}$$
$$\dot{\mathbf{C}}_\pm = -\mathbf{C}_\pm \mp \mathsf{B}^0 g_\pm(\mathbf{C}) + \mathsf{Q}\mathbf{E}_\pm - \mathsf{H}\mathbf{L}_\pm,$$

where $g_\pm(\mathbf{C}) = [g_C(\mathbf{C}_l) - g_c(\bar{\mathbf{C}})] \pm [g_C(\mathbf{C}_r) - g_c(\bar{\mathbf{C}})]$. If the nonlinearity is of the form $g_C(x + \bar{\mathbf{C}}) - g_C(\bar{\mathbf{C}}) = x + ax^2 - bx^3 + \mathcal{O}(x^4)$, we have

$$g_-(\mathbf{C}) \approx C_- + aC_+C_- - bC_-^3/4 - 3bC_-C_+^2/4,$$
$$g_+(\mathbf{C}) \approx C_+ + aC_+^2/2 + aC_-^2/2 - bC_+^3/4 - 3bC_+C_-^2/4.$$

Hence, when $C_- = 0$, C_+ cannot excite it since $g_-(\mathbf{C}) = 0$. However, if $a \neq 0$, the synchronous mode will be excited passively by the antiphase mode through the quadratic coupling term $aC_-^2/2$, responding with double frequency, as could be tested easily.

To analyze coupling between the antiphase modes, we assume for simplicity that $g_c(x + \bar{\mathbf{C}}) - g_c(\bar{\mathbf{C}})$ is odd in x, so $C_+ = 0$ since the synchronous mode is damped, and $g_-(C_-) = 2g_C(C_-/2)$. Consider a small perturbation, in the m' mode direction, to the $m = 1$ cycle (the final orbit resulting from a small deviation from the fixed point in the $m = 1$ mode, with a fundamental harmonic in the $m = 1$ mode) such that $\mathbf{C}_-(x) \approx C_1 \cos(2\pi x/N) + C_{m'}\cos(2\pi m'x/N)$, with $C_{m'} \ll C_1$. Expressing $g_-(\mathbf{C})$ as $g_-(\mathbf{C}) = \sum_n g_n e^{i2\pi nx/N}$, it can be shown that for large N, $g_{m'} \approx C_{m'}\bar{g}_C'$ where $\bar{g}_C'$ is the derivative of g_C averaged over the unperturbed cycle. (More details will be given in a future paper.) Because of the sigmoid form of $g_C(C)$, $\bar{g}_C' < g_C'(\bar{C})$. Then $C_{m'} \propto e^{\lambda_m^- t}$ with $\lambda_{m'}^-$ as in Eq. (4) except that $(B_{m'}, K_{m'})$, values derived from connections from $\mathbf{C}$ cells, are rescaled by a factor $\bar{g}_C'/g_C'(\bar{C}) < 1$. Thus the swimming cycle at large amplitude remains stable against perturbation in other modes, even when the fixed point is unstable against these perturbations.

If $\mathrm{Re}(\lambda_1^-) \gg \mathrm{Re}(\lambda_{m'}^-) \gtrsim 0$, the m' cycle will have a small amplitude and hence $\bar{g}'(C) \sim g'(\bar{C})$, and it will be unstable against perturbation in the $m = 1$ mode. For larger $\mathrm{Re}(\lambda_{m'}^-)$ the amplitude of the cycle is larger and either cycle will be stable. Suppose the neural connections are such that the $m = \pm 1$ cycles, giving forward or backward swimming, are both stable. The system would then display hysteresis, with the final behavior depending on the initial conditions. Forward or backward swimming could then be selected by transient inputs from the brain stem, rather than by setting constant inputs as described above. This seems less likely to be the actual selection mechanism since experiments on fictive swimming (presumably with random initial conditions) seldom observe spontaneous backward swimming. However, the forward swimming could simply have a larger basin of attraction than backward swimming.

When the lamprey turns, average neural activities on the left and the right sides are unequal. This is realizable by adding an additional constant input to one side in the animal and in models [8,9]. This does not disrupt the oscillations provided that the gains $g'(\cdots)$ are roughly constant near the fixed points. Simulations (Fig. 2) confirm the analysis above.

To study behavior at the body ends or in short sections of the spinal cord [1], or equivalently to see the effects of longer connections, we abandon translation invariance. Eliminating $\mathbf{C}$ in Eq. (3), the minus mode has

$$\ddot{\mathbf{E}} + (2 - \mathsf{J} - \mathsf{B})\dot{\mathbf{E}} + [1 - \mathsf{J} - \mathsf{B} + \mathsf{BJ} + \mathsf{K}(\mathsf{H} - \mathsf{Q})]\mathbf{E} = 0,$$

or oscillator i is driven by force F_i from other oscillators,

$$\ddot{\mathbf{E}}_i + (2 - \mathsf{J}_{ii} - \mathsf{B}_{ii})\dot{\mathbf{E}}_i + [1 - \tilde{\mathsf{R}}_{ii}]\mathbf{E}_i = F_i \equiv \sum_{j \neq i} F_{ij} \equiv \sum_{j \neq i} (\mathsf{J}_{ij} + \mathsf{B}_{ij})\dot{\mathbf{E}}_j + \sum_{j \neq i} \tilde{\mathsf{R}}_{ij}\mathbf{E}_j,$$

where $\tilde{\mathsf{R}} = \mathsf{B} + \mathsf{J} - \mathsf{BJ} - \mathsf{K}(\mathsf{H} - \mathsf{Q})$. The intrinsic oscillation, $\mathbf{E}_i \sim e^{\lambda t}$, is damped, $\mathrm{Re}(\lambda) = -1 + (\mathsf{J} + \mathsf{B})_{ii}/2 < 0$, as indicated by experiments [1,2]. We estimate F_i using the approximation that oscillators $j \neq i$ still behave as $\mathbf{E}_j \propto e^{-i(\omega t - kj)}$. We then have $F_i = \alpha_i \dot{\mathbf{E}}_i + \beta_i \mathbf{E}_i$, where

$$\alpha_i \equiv \sum_{j \neq i} \{(\mathsf{J} + \mathsf{B})_{ij} \cos[k(j - i)] - \tilde{\mathsf{R}}_{ij} \sin[k(j - i)]/\omega\},$$

$$\beta_i \equiv \sum_{j \neq i} \{(\mathsf{J} + \mathsf{B})_{ij} \omega \sin[k(j - i)] + \tilde{\mathsf{R}}_{ij} \cos[k(j - i)]\}.$$

The term $\alpha_i \dot{\mathbf{E}}_i$ when $\alpha_i > 0$ feeds oscillation energy into the ith (receiving) oscillator, causing emergent oscillations in coupled damped oscillators. We divide $\alpha_i = \alpha_{i,\mathrm{desc}} + \alpha_{i,\mathrm{asc}}$ into the descending and ascending parts, with summations over $\sum_{j<i}$ and $\sum_{j>i}$, respectively. Hence, for $i = 1$, $\alpha_1 = \alpha_{i,\mathrm{asc}}$, for $i = N$, $\alpha_N = \alpha_{i,\mathrm{desc}}$, and for $1 \ll i \ll N$, $\alpha_i = \alpha_1 + \alpha_N$. Since the first and last segments oscillate due to the driving force from other oscillators, $\alpha_1 > 0$ and $\alpha_N > 0$. Consequently, $\alpha_1 < \alpha_{N/2}$

and $\alpha_N < \alpha_{N/2}$. Further, since descending connections are stronger, it is most likely that, for $1 \ll i \ll N$, $\alpha_{i,\mathrm{desc}} > \alpha_{i,\mathrm{asc}}$. Consequently, $\alpha_1 < \alpha_N$. Hence, the rostral oscillator has a smaller amplitude than the caudal one, which in turn has a smaller amplitude than the central one [Fig. 2(e)]. Firing rate saturation and variations of the fixed point along the body may obscure this pattern in experimental data, although body movements are indeed smallest near the head [10]. Similarly, oscillation amplitudes will be reduced in sections of spinal cords shorter than the typical lengths of intersegment connections, and will eventually be zero in ever shorter sections, as observed in experiments [2].

In summary, analysis of a model of the CPG neural circuit in lampreys has given new insights into the neural connection structures needed to generate and control the swimming behavior. In particular, we predict that the contralateral connections between $\mathbf{C}$ must be stronger than the self-excitatory connection strength of the $\mathbf{E}$ neurons, that the $\mathbf{C}$ neurons are more inhibited (in their ac components) by $\mathbf{L}$ neurons than excited by the $\mathbf{E}$ neurons, and we have shown how different swimming regimes can be selected by scaling the strengths of the various neural connections without changing the connection patterns. Our framework should help to provide further insights into CPGs of animal locomotion.
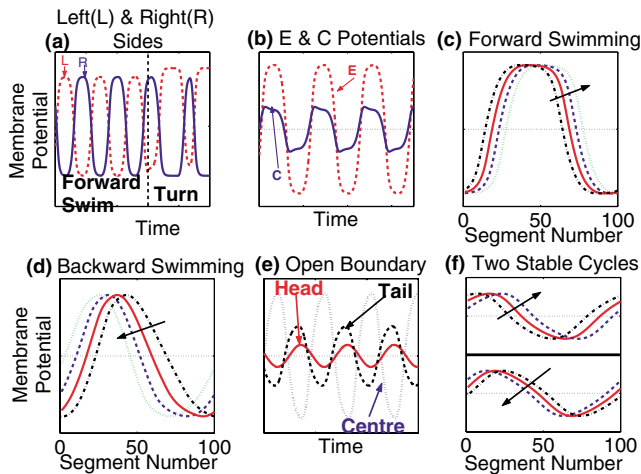
FIG. 2 (color online). Simulations. (a) Membrane potentials of $\mathbf{E}$ population on either side of one segment during forward swimming and turning. Turning is induced by an additional constant input to one side only, starting at the time indicated by the dashed line. (b) $\mathbf{C}$ slightly phase leads $\mathbf{E}$ during forward swimming. (c),(d) Waveform of $\mathbf{E}$ along the body in forward and backward swimming, at consecutive times increasing in the direction indicated by the arrows, in the translational invariant model. The switch from forward to backward swimming is achieved by increasing the strength of H and Q. (e) Oscillation waveforms (note different amplitudes) in body segments at head, tail, and center of the body, without translational invariance. (f) Forward and backward swimming from different initial conditions, with the same connection strengths and inputs.

[1] S. Grillner and P. Wallen, Brain Res. Rev. **40**, 92 (2002).
[2] J.T. Buchanan, Prog. Neurobiol. **63**, 441 (2001); J. Neurophysiol. **81**, 2037 (1999).
[3] A. D. McClellan and A. Hagevik, Exp. Brain Res. **126**, 93 (1998).
[4] A. H. Cohen, P. J. Holmes, and R. H. Rand, J. Math. Biol. **13**, 345 (1982).
[5] G. B. Ermentrout and N. Kopell, Commun. Pure Appl. Math. **30**, 623 (1986); N. Kopell and G. B. Ermentrout, SIAM J. Appl. Math. **54**, 478 (1994); N. Kopell and G. B. Ermentrout, SIAM J. Appl. Math. **50**, 1014 (1990).
[6] D. Taylor and P. Holmes, J. Math. Biol. **37**, 419 (1998).
[7] R. Jung, T. Kiemel, and A. H. Cohen, J. Neurophysiol. **75**, 1074 (1996).
[8] A. K. Kozlov, F. Ullen, P. Fagerstedt, E. Aurell, A. Lansner, and S. Grillner, Biol. Cybern. **86**, 1 (2002).
[9] A. D. McClellan and A. Hagevik, J. Neurophysiol. **78**, 214 (1997).
[10] K. C. Paggett, V. Gupta , and A. D. McClellan, Exp. Brain Res. **119**, 213 (1998).